Acta Geochim (2016) 35(4):329–339
DOI 10.1007/s11631-016-0119-1

ORIGINAL ARTICLE

Fractionation characteristics of rare earth elements (REEs) linked with secondary Fe, Mn, and Al minerals in soils

Chunying Chang[1,3] · Fangbai Li[1] · Chengshuai Liu[1,2] · Jianfeng Gao[2] · Hui Tong[2] · Manjia Chen[1]

Received: 16 June 2016 / Revised: 24 July 2016 / Accepted: 15 August 2016 / Published online: 27 August 2016

Abstract Soil secondary minerals are important scavengers of rare earth elements (REEs) in soils and thus affect geochemical behavior and occurrence of REEs. The fractionation of REEs is a common geochemical phenomenon in soils but has received little attention, especially fractionation induced by secondary minerals. In this study, REEs (La to Lu and Y) associated with soil-abundant secondary minerals Fe-, Al-, and Mn-oxides in 196 soil samples were investigated to explore the fractionation and anomalies of REEs related to the minerals. The results show right-inclined chondrite-normalized REE patterns for La–Lu in soils subjected to total soil digestion and partial soil extraction. Light REEs (LREEs) enrichment features were negatively correlated with a Eu anomaly and positively correlated with a Ce anomaly. The fractionation between LREEs and heavy REEs (HREEs) was attributed to the high adsorption affinity of LREEs to secondary minerals and the preferred activation/leaching of HREEs. The substantial fractions of REEs in soils extracted by oxalate and Dithionite-Citrate-Bicarbonate buffer solutions were labile (10 %–30 %), which were similar to the mass fraction of Fe (10 %–20 %). Furthermore, Eu was found to be more mobile than the other REEs in the soils, whereas Ce was less mobile. These results add to our understanding of the distribution and geochemical behavior of REEs in soils, and also help to deduce the conditions of soil formation from REE fractionation.

Keywords Rare earth elements · Fractionation · Secondary minerals · Geochemical process · Europium anomaly · Cerium anomaly

1 Introduction

The rare earth elements (REEs) are group IIIB members of the periodic table and behave in a consistent manner in the environment because of their common electron configuration consisting of six shells, large ionic radii and (III)-oxidation states (Henderson 1984). REEs are considered excellent environmental tracers and have been widely used to probe the chemical evolution of the earth surface environment (McLennan 1989; Yan et al. 2012; Migaszewski et al. 2015; Singh and Rajamani 2001), chemical weathering in drainage basins (Nesbitt 1979), paleoenvironmental changes in the oceans (Holser 1997), and sediment sources (provenance) and tectonic setting (Cullers et al. 1987). The abnormal geochemical behavior of individual REEs usually results from specific environmental conditions or special geologic bodies (Nesbitt 1979; Daux et al. 1994). Exploring the distribution and geochemical properties of REEs, especially the common REEs Ce and Eu, is therefore helpful in deducing the evolution of the earth surface environment (Lee et al. 2003; Liu et al. 2015).

Electronic supplementary material The online version of this article (doi:10.1007/s11631-016-0119-1) contains supplementary material, which is available to authorized users.

✉ Chengshuai Liu
liuchengshuai@vip.gyig.ac.cn

[1] Guangdong Key Laboratory of Agricultural Environment Pollution Integrated Control, Guangdong Institute of Eco-Environmental and Soil Sciences, Guangzhou 510650, China

[2] State Key Laboratory of Environmental Geochemistry, Institute of Geochemistry, Chinese Academy of Sciences, Guiyang 550081, China

[3] Guangdong Key Laboratory of Contaminated Sited Environmental Management and Remediation, Guangdong Provincial Academy of Environmental Science, Guangzhou 510045, China

REEs in soils mainly originate from soil parental rocks, some of which have high REE content (Clark 1984; Kanazawa and Kamitani 2006; Berger et al. 2014; Mongelli et al. 1996). Minerals with a high REE content are more likely to control the REE signature of the parent rock as well as the subsequent secondary minerals (Laveuf and Cornu 2009). REEs in secondary minerals behave differently from those in primary minerals; studies about REE accumulation and fractionation in secondary minerals have attracted more attention. REE redistribution during weathering is dependent on natural primary rocks, properties of the secondary minerals or soils, and the degree of soil weathering (Hedrick 1995; Laveuf and Cornu 2009; Caggianelli et al. 1992). When released from primary rocks, REEs are either lost into the soil solution from the weathering profile or incorporated into secondary minerals (Öhlander et al. 1996; Kissao and Heinz 2003; Laveuf and Cornu 2009). REEs generally decrease with increasing degrees of weathering (Clark 1984; Taunton et al. 2000), and are removed from the upper profile, transferred downwards, and then precipitated in the base profile (Wayne and Markovics 1997; Feng 2010).

Once they are incorporated into soil secondary minerals after soil formation, REEs migrate through the weathering profile based on both their relative solubility and mobility and the properties of the secondary minerals. A variety of factors have been reported to influence the retention of mobile REEs including soil composition (Gruau et al. 2004), water–rock interactions (Takahashi et al. 2002), solution complexation (Leybourne and Johannesson 2008; Ohta and Kawabe 2001), and biological activity (Brioschi et al. 2013; Šmuc et al. 2012).

Secondary minerals, including Fe- and Mn-oxides, are recognized as important REE scavengers (Galán et al. 2007; Öhlander et al. 1996; Yusoff et al. 2013) and can fractionate REEs through a variety of geochemical processes, particularly surficial sorption (López et al. 2005; Sanematsu et al. 2013). REE behavior in surface soils is closely related to interactions with secondary minerals, especially geochemically active secondary minerals such as Fe-, Al-, and Mn-oxides (Babechuk et al. 2014; Ndjigui et al. 2008). Furthermore, the distribution and fractionation of REEs are highly variable in different soils due to variations in secondary minerals (Galán et al. 2007; Yusoff et al. 2013). Particularly, soils in tropical and subtropical regions are undergoing continuous active geochemical reactions after soil formation due to hot and humid climates (Gurumurthy et al. 2015; Ettler 2016). The soil secondary minerals in these regions have a strong effect on the geochemical properties of soil elements, including REEs (Ren et al. 2015). However, studies on the fractionation of REEs related to secondary minerals are rarely reported; in particular, the mechanisms of active secondary minerals on the fractionation of REEs in soils are still poorly understood.

In this study, therefore, we focused on exploring the fractionation characteristics of REEs that are traceable to secondary minerals, especially the abundant minerals of Fe-, Al-, Si-, and Mn-oxides in soils. In total, 196 soil samples of alluvium were collected in the Pearl River Delta (PRD) region, where the warm-wet climate and river networks are representative of river delta areas elsewhere in the world. Based on studying the fractionation characteristics of REEs associated with soil minerals, the aims of the present study were to (i) assess the characteristics of mobility and fractionation of soil REEs in the river delta, and (ii) explore the mechanisms that may be responsible for the mobility and fractionation of REEs during weathering processes in the soils.

2 Materials and methods

2.1 Study area description and sampling locations

The studied area is situated in the southeastern Guangdong Province, China, at 23°40′−21°30′N latitude and 112°−115°30′E longitude (Fig. 1). One of the most developed regions in China, the PRD is also an important agricultural area. The region produces large amounts of vegetables and fruits to supply the Chinese mainland, Hong Kong, and Macao (Xing et al. 2012). The PRD region has a complicated topography including mountains, hilly regions, and plateaus. Soils in the PRD region were primarily formed from river alluvium of the Pearl River and its tributaries. One hundred and ninety-six soil samples were collected from the surface horizon (0–20 cm) with a bamboo shovel in April to November of 2012 throughout

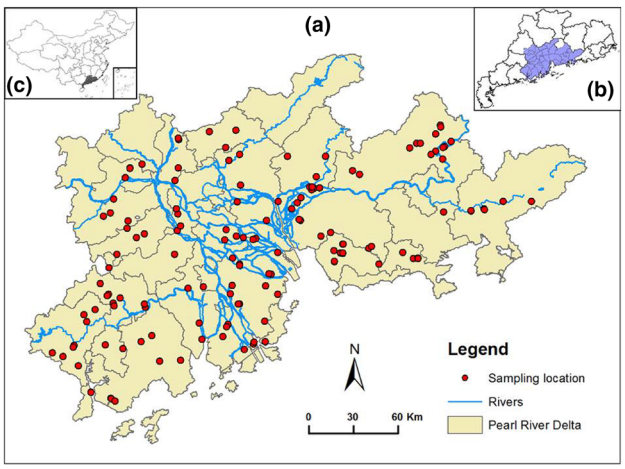

Fig. 1 Map of the sampling locations in the Pearl River Delta (PRD) region (**a**). PRD is located in Guangdong Province (**b**) of China (**c**)

the PRD (Fig. 1). All the sampling locations were far from urban and industrial areas to avoid the effect of human activity. All collected samples were sealed in polyethylene bags and pretreated within 6 h of collection.

2.2 Analyses of soil properties and REEs

Visible plant debris and impurities in the soils were manually removed, and then the soils were air-dried at room temperature. After being ground with an agate mortar, the soils were passed through an 80 mesh (0.2 mm) sieve. The soil pH (H_2O) and pH (KCl) were measured in soil slurries at a soil-to-water and soil-to-KCl solution (1 M) ratio of 1:2.5 with a calibrated PHS-3C pH meter (Sartorius, China). Soil organic matter (OM) contents were determined by the $K_2Cr_2O_7$–H_2SO_4 oxidation method (Pansu and Gautheyrou 2006). Soil texture analyses (clay <0.002 mm, silt 0.05–0.002 mm, and sand 2.00–0.05 mm) were conducted by the pipette method (Soil Survey Staff 2004).

Partial extractions of soil Fe, Al, Si, and Mn were performed sequentially with oxalic acid-ammonium oxalate (Oxalate, pH 3.2) and dithionite-citrate-bicarbonate (DCB) buffer solutions (Mehra and Jackson 1958; Schwertmann 1964). Fe, Al, and Mn contents of the extract solutions were determined by WFX-130 flame atomic absorption spectrophotometer (Braic, China). Silicon contents of extract solutions were determined by the silicon–molybdenum blue colorimetric method on a UV spectrophotometer (TU-800, Beijing, China). The oxalate solution can extract the physically adsorbed parts and chemical bonding portion of soil Fe, Mn, or Al that bind with mineral particles when hydroxy-hydrated with clay particles. DCB-extractable Fe, Mn, and Al mainly exist in the oxidation, amorphous, and crystalline states in soils (Peretyazhko and Sposito 2005).

Total Fe, Al, Ca, Mg, K, and Na contents were measured on an inductively coupled plasma-atomic emission spectrometer (ICP-AES, Optima 3300 DV, Perkin Elmer, USA) after the soils had been digested with HNO_3–$HClO_4$–HF (Pansu and Gautheyrou 2006). The total Si contents were determined using the silicon–molybdenum blue colorimetric method on the UV spectrophotometer. Total Fe, Si, Al, Ca, Mg, K, and Na contents in the soils were measured as mol/kg of soil as Fe_2O_3, SiO_2, Al_2O_3, CaO, MgO, K_2O, and Na_2O. The properties and the obtained mineral contents are provided in Supplementary material Table S1.

Total REE contents of the soils were determined according to the method described by Li et al. (2008). In brief, 600 mg of air-dried soil was mixed with 6 mL of concentrated HNO_3–$HClO_4$ (87:13, v/v) and 6 mL of concentrated HF (mass fraction >40 %). The mixture was digested and then dissolved in 15 mL 2 % HCl solution. For soil secondary minerals, the partial extractions of soil REEs were performed with oxalate and DCB solutions separately. The REE contents of digestion and extraction solutions were determined by inductively coupled plasma mass spectrometry (ICP-MS, NX300, PerkinElmer, USA). Soil reference materials of GBW07423 (GSS-9), GBW 07428 (GSS-14), and GBW07429 (GSS-15) were analyzed as quality control. Precision and accuracy of REE were better than 5 %.

2.3 Data analyses

Statistical analyses were performed with SPSS 13.0. The primary geochemical factors that influence REE distribution and fractionation were investigated by using the two-tailed Pearson correlation analysis (PCA) (with significance levels at $p < 0.05$ and $p < 0.01$) and principal component analysis. The REE group can be separated into two sub-groups, i.e., the LREEs and the HREEs. Some ratios such as ΣCe/ΣY, $(Gd/Yb)_N$, $(La/Sm)_N$, Eu/Eu* and Ce/Ce* can be used to describe the REE fractionation characteristics and quantitative characterization. These parameters are calculated as follows:

$$\sum Ce / \sum Y = \frac{\sum (\mathrm{La} + \mathrm{Ce} + \mathrm{Pr} + \mathrm{Nd} + \mathrm{Sm} + \mathrm{Eu})}{\sum (\mathrm{Gd} + \mathrm{Tb} + \mathrm{Dy} + \mathrm{Ho} + \mathrm{Er} + \mathrm{Tm} + \mathrm{Yb} + \mathrm{Lu} + \mathrm{Y})} \quad (1)$$

$$(Gd/Yb)_N = \frac{Gd_{norm}}{Yb_{norm}} \quad (2)$$

$$(\mathrm{La/Sm})_N = \frac{\mathrm{La}_{norm}}{\mathrm{Sm}_{norm}} \quad (3)$$

$$\frac{\mathrm{Ce}}{\mathrm{Ce}^*} = \frac{\mathrm{Ce}_{norm}}{\sqrt{\mathrm{La}_{norm} \times \mathrm{Pr}_{norm}}} \quad (4)$$

$$\frac{\mathrm{Eu}}{\mathrm{Eu}^*} = \frac{\mathrm{Eu}_{norm}}{\sqrt{\mathrm{Sm}_{norm} \times \mathrm{Gd}_{norm}}} \quad (5)$$

where the subscripts (*norm*) indicate the chondrite-normalized contents of REEs. The chondrite data are from a previous report (Boynton 1984).

3 Results

3.1 Total REEs in the soils

The contents of REEs—La to Lu and Y—in the soils are shown in Table S2. The REE contents in the soils obey the Oddo-Harkins rule (the odd–even effect) (Wei et al. 2001), i.e., REEs with even atomic numbers were detected at higher levels than those with odd atomic numbers. The

REE contents of different soils were differentiated, and the sum of the REEs (ΣREE), LREEs (ΣCe or ΣLREE), and HREEs (ΣY or ΣHREE) ranged between 37–550, 32–480, and 4.8–128 mg/kg, with means of 268, 210, and 58 mg/kg, respectively. ΣCe accounted for approximately 80 % and ΣY accounted for approximately 20 % of the total REEs in all soils. A statistical analysis of the frequency of REE contents in the soils showed that ΣREE was consistent with a normal distribution, and the peak values ranged from 200 to 250 mg/kg.

The soils in the PRD region typically have relatively smooth REE patterns when normalized to chondrite, except for an obvious depression between LREEs and HREEs (Fig. 2). A subtle REE fractionation in the soils, however, was apparent from the chondrite-normalized plots. For example, there was an LREE-enrichment as illustrated by the average $(La/Sm)_N$ of 3.98 (range 2.71–5.68, n = 196; all samples have values > 1.00) (Fig. 2 and Fig. 3i). In addition, more than 80 % of the soil samples were clearly enriched with LREEs, exhibiting concave-up and chondrite-normalized patterns with $(Gd/Yb)_N > 1$ (Figs. 2, 3j). Most sedimentary soils were characterized by a slightly positive Ce anomaly and a strongly negative Eu anomaly (Figs. 2, 3k, l) in which Ce/Ce* and Eu/Eu* ranged from 0.59 to 2.65 (mean of 1.13) and 0.17 to 0.79 (mean of 0.55), respectively.

3.2 Partial REE extraction from soils

The results from partial extractions, i.e., soils extracted with oxalate and DCB separately, exhibited highly variable

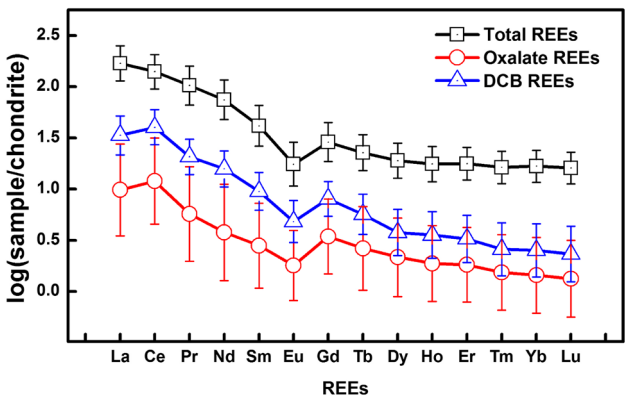

Fig. 2 Chondrite-normalized REE distribution patterns in the studied soils. Chondrite Composite was used for normalization, and its REE values (in ppm) are as follows: La 0.310; Ce 0.808; Pr 0.122; Nd 0.60; Sm 0.195; Eu 0.0735; Gd 0.259; Tb 0.0474; Dy 0.322; Ho 0.0718; Er 0.210; Tm 0.0324; Yb 0.209; and Lu 0.0322 (Boynton 1984). The oxalate- and DCB-extracted REE contents were extracted with oxalic acid-ammonium oxalate (pH 3.2) and dithionite-citrate-bicarbonate buffer solutions (DCB), respectively

REE concentrations across soils (Table S2). The ΣREE, ΣLREE, and ΣHREE ranged 1.45–64 mg/kg (mean 23.5 mg/kg, n = 196), 0.85–71 mg/kg (mean 20.7 mg/kg), and 0.59–21.1 mg/kg (6.9 mg/kg) in the oxalate extract, respectively. For the DCB-extracted REE contents, the ΣREE, ΣLREE, and ΣHREE ranged 10.2–174 mg/kg (mean 72 mg/kg, n = 196), 8.6–138 mg/kg (mean 58 mg/kg), and 1.63–37 mg/kg (mean 14.1 mg/kg), respectively. The contents of DCB-extracted LREEs and HREEs were clearly higher than those of oxalate-extracted soils (Fig. 3).

The partial extractions were also commonly enriched with LREEs to a critical extent compared with that of the total soil digestion, with an average $(La/Sm)_N$ value of 3.22 (ranging from 0.92 to 13.6, n = 169, with only one sample having a value lower than 1) when extracted with oxalate, and of 3.38 (ranging from 1.95 to 6.51) when extracted by DCB (Fig. 3i). Similarly, the majority of the oxalate and DCB extractions were enriched with LREEs, with an average $(Gd/Yb)_N$ value of 3.24 (ranging from 0.82 to 9.32, with only 4 samples having values lower than 1) and 3.28 (ranging from 1.58 to 6.87, with no samples lower than 1), respectively (Fig. 3j). Consistent with the total REEs in soils, the REEs in the oxalate and DCB extractions both were characterized by slightly positive Ce- and clearly negative Eu- anomalies. The Ce/Ce* and Eu/Eu* contents in oxalate extracts ranged from 0.46 to 6.71 (mean of 1.87) and 0.15 to 1.62 (mean of 0.58), and ranged from 0.85 to 5.66 (mean of 1.65) and 0.20 to 0.92 (mean of 0.60) in the DCB extracts, respectively. The LREEs are generally more enriched in the oxalate and DCB extracts than the LREEs of the total soil digestion. In comparison with the total analyses, the Ce and Eu anomalies were also generally more enriched (both positively and negatively) in the partial extracts (Figs. 2, 3).

As shown in the lognormal probability plots (Fig. 3), the relationships between the total contents and partial-extraction contents of REEs differed for different elements. More than 64.8 % of the Mn was extracted by DCB solution, whereas approximately 21.1 % of the Fe and only 1.68 % of the Al were extracted. Thus, Mn primarily exists in the soils in readily labile forms, including adsorbed forms and poorly crystalline Mn (hydr)oxide coatings (Tani et al. 2003; Braun et al. 1998), or incorporated/co-precipitated forms in the Fe (hydr)oxide mineral coatings (Leybourne 2001). Most of the Fe (78.9 %) and Al (98.3 %) in soils are dominant compositions of soil minerals, including Fe and Al oxides. Furthermore, the cumulative frequency plots of REEs, including LREEs, HREEs, Eu, and Ce, were more similar to that of Fe rather than Mn, Al, and Si.

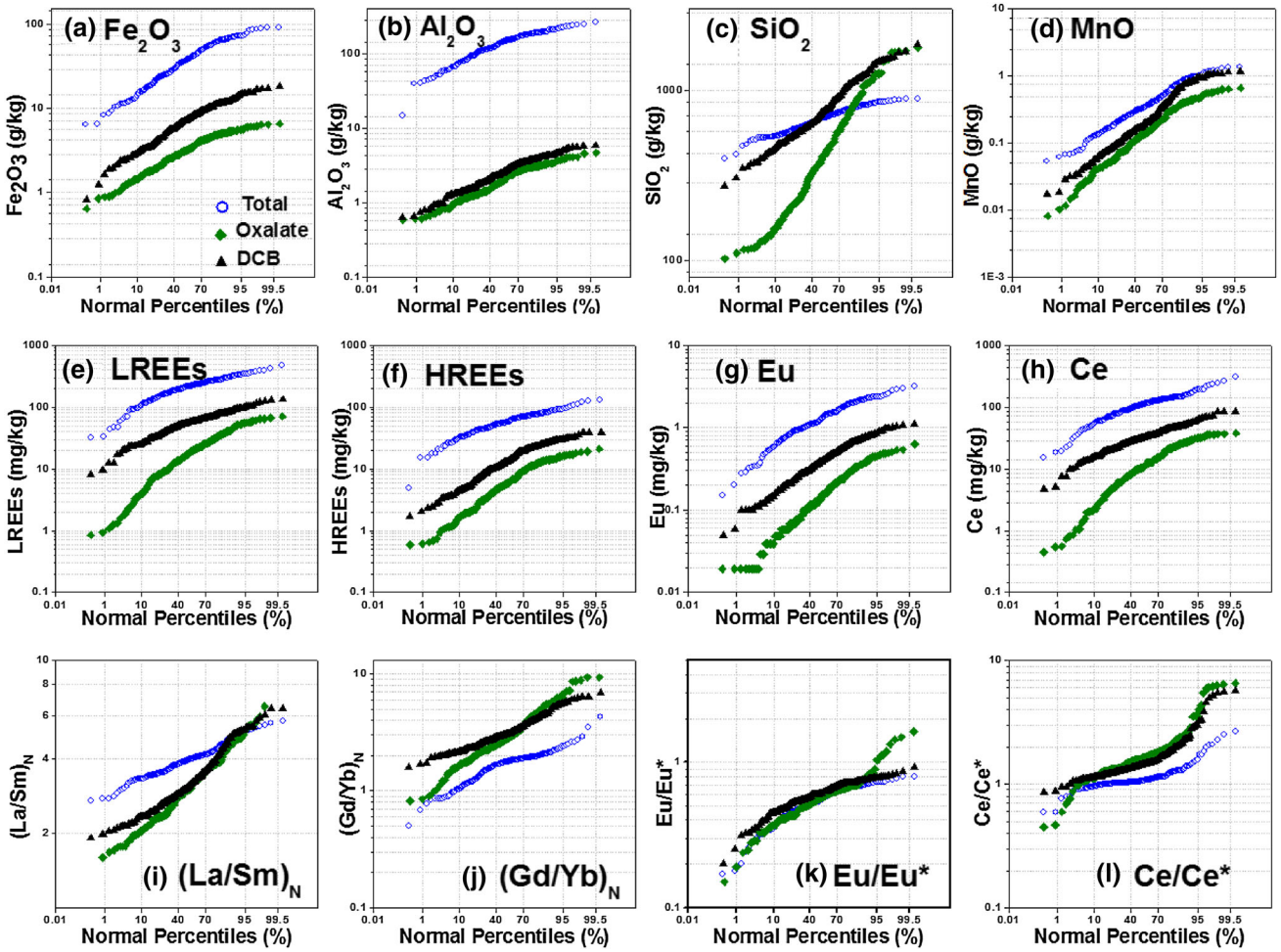

Fig. 3 Log-normal probability plots for the total digestion, oxalate- and DCB-extracted from the soils for Fe_2O_3, Al_2O_3, SiO_2, MnO, and selected REEs. Probability plots for the selected chondrite-normalized REE ratios are also included

The average values of the LREEs/HREEs (ΣCe/ΣY) ratio in soils of total digestion, oxalate, and DCB extracts were all higher than 1 (3.75, 2.78, and 5.02, respectively), which suggests a strong fractionation between LREEs and HREEs. The average ratio values of $(Gd/Yb)_N$ for soils of total digestion, oxalate, and DCB extracts were 1.36, 3.24, and 3.28, respectively, which indicates easier mobility for the oxalate- and DCB-extracted REEs. The average ratio values of $(La/Sm)_N$ were 3.98, 3.22, and 3.38 for the total digestion, oxalate, and DCB extracts, respectively, indicating a stronger LREE enrichment than that of HREE in the soils. The average Eu/Eu* values were 0.55, 0.58, and 0.60 for the total digestion, oxalate, and DCB extracts, respectively, reflecting a strong negative Eu anomaly (<1) (Table S1). Deep Eu "depression" was also indicated in the patterns of chondrite-normalized REEs (Fig. 2). The average Ce/Ce* values in soils showed a slight positive Ce anomaly (>1), with the total digestion, oxalate-, and DCB-extracted REEs of 1.13, 1.87, and 1.65, respectively.

4 Discussion

4.1 REE fractionation patterns in the soils

REE fractionation usually occurs in soils during soil geochemical processes, such as oxidation–reduction, hydrolysis reactions, and adsorption–desorption reactions, and also depends on the physicochemical properties of REEs (Ma et al. 2011; Banfield and Eggleton 1989; Nesbitt 1979). Chondrite-normalized REE distribution patterns (except for Y) can represent the characteristics of REE fractionation in soil weathering processes.

REEs in total soil digestion and soil extracts of oxalate and DCB exhibited similar chondrite-normalized patterns of LREE enrichment with a clearly negative Eu anomaly. The pattern of normalized REEs for the total soils was parallel to but higher than the REEs in the oxalate and DCB extracts (Fig. 2). A comparison of the REE patterns between the total soil digestion and those in the partial extracts showed that total REEs in soils are typically more

enriched with LREEs (except for Eu) than that in the oxalate or DCB extracts (Fig. 2; Table S1). The oxalate solution can generally extract the physically adsorbed parts and the chemical bonding portion of soil REEs that bound with amorphous oxides in soils. The DCB-extractable portions of soil REEs contain the REEs on/in amorphous and crystalline soil minerals. The partial extracts, which primarily include the labile and amorphous Fe/Mn (hydr)oxides in the sediments, were less enriched with LREEs compared with the total REEs in soils.

PCA applied to major soil elements and REEs can help to evaluate the spatial representation of the association among these elements. The PCA results of the REE distribution and soil properties are shown in Table S3 and 4. The total REEs (ΣREE, ΣLREE, and ΣHREE) did not correlate with either the soil pH (H_2O) or pH (KCl). This result is consistent with previous reports of REEs in the red soils of southern China (Yang et al. 2004). Some researchers, however, consider that soil pH is an important factor affecting the distribution of REEs, and a suitable soil pH can be used to determine the strength of chemical bonds relating to REEs (Marsac et al. 2013; Zhu and Xing 1992). Most of the soils in the present study were acidic, and some regions were even severely acidified. The pH (H_2O) and pH (KCl) values varied between 3.86–8.07 and 3.26–7.36, with mean values of 6.22 and 5.66, respectively, and with 152 and 185 samples returning less than the neutral pH of 7.0. Excessive acidification conditions of soils therefore may obscure the influences of soil pH on REE distribution. The soil OM was significantly correlated with HREEs in both total digestion and partial extracts (Table S3). These results indicate that soil OM slightly impacted REE enrichment, and preferentially impacted HREEs, through adsorption because of their mobility (Sonke 2006; Davranche et al. 2004). The $(La/Sm)_N$ in total digestion and DCB extracts consistently exhibited a significant negative correlation with soil OM ($p < 0.01$), and the $(Sm/Nd)_N$ showed a positive and significant ($p < 0.01$) correlation with soil OM, which also indicated preferential adsorption of HREEs. A large number of carboxyl groups, phenolic hydroxyl groups, and N- and S-binding sites have been reported on soil OM structures and are thought to be easily combined with rare earth ions (REE^{3+}) (Chen et al. 1996; Marsac et al. 2013), affecting the migration and biological activity of REEs in the environment. Although the REE complexing mechanisms with soil OM require further investigation, our findings indicate that the primary integration positions of REEs on OM were organic weak acid complexation, carboxyl-COOH, and phenolic hydroxyl-OH (Pourret et al. 2007). The soil CEC and contents of sand and silt all showed significant correlation mostly at the 0.01 level mostly and some at the 0.05 level with REEs (ΣREE, ΣLREE, and ΣHREE) in both total digestion and partial extracts. The high correlations ($p < 0.01$) between soil CEC and REEs suggest consistent enrichment in the soils (López et al. 2005). The correlation between the soil texture and REE concentrations indicate that REEs (both LREEs and HREEs) tend to be hosted in the finer particles, which is primarily attributed to the strong adsorption of REEs on minerals through hydroxyl-hydrated sites (Laveuf and Cornu 2009).

The PCA results for Fe, Al, Mn, Si, and REE contents are shown in Fig. 4. The REEs in PCA describe an arc or a 'horseshoe curve' ordered by the atomic number (except for Ce and Eu) (Marmolejo-Rodríguez et al. 2007). The inclusion of Si in the analysis made the 'horseshoe curve' transpose completely along the X-axis. Moreover, the LREEs and HREEs exhibited obvious fractionation (with Gd as a transitional element) along the $Y = 0$ line. The Ce and Eu anomalies also deviated from the 'horseshoe curve.' The soil Si contents show different associations with REEs (Fig. 4). On the contrary, REEs were significantly correlated with soil Fe and Mn, while moderately correlated with Al content. Consistent results for the correlations between REEs and Fe, Al, Si, or Mn in soil can also be obtained by analyzing the lognormal probability plots (Fig. 3).

These relationships can also be found in PCA of soil major elements and REEs (Table S3). Significantly positive correlations ($p < 0.01$) were found between the oxalate-extracted REEs and total digested REEs, with R of 0.557 for HREEs and 0.630 for LREEs, indicating considerable amounts of exchangeable REEs in the soils. Total REEs in the soils showed a strong correlation with the soil Fe-, Al-, and Mn-oxide contents although largely varied with different oxides forms, but showed a weak correlation with soil Si contents. The weak correlation between REEs and Si content was also confirmed by the cumulative plots of REEs in partial extracts and the total soil Si contents when compared with selected REEs (Fig. 3). Total soil Fe, oxalate-Fe, and DCB-Fe all showed significant correlations with HREEs ($p < 0.01$), and the correlations between soil Fe and LREEs were even better (Fig. 4 and Table S4), which indicates that Fe-bearing minerals had a stronger holding capability for LREEs than that of HREEs. These results are consistent with those reported previously by Tang et al. (2002), who studied the relationship between Fe oxide and REEs in paddy soils and found that the combined REEs from soil amorphous-Fe (oxalate-Fe) and crystal-Fe were primarily LREEs.

Soil secondary minerals, especially Fe-, Al-, and Mn-oxides, are important scavengers for REEs and can also fractionate REEs during soil geochemical processes (Ren et al. 2015). The distribution characteristics of REEs between labile and non-labile phases in soils from PRD regions were more similar for Fe minerals than for Mn, Al,

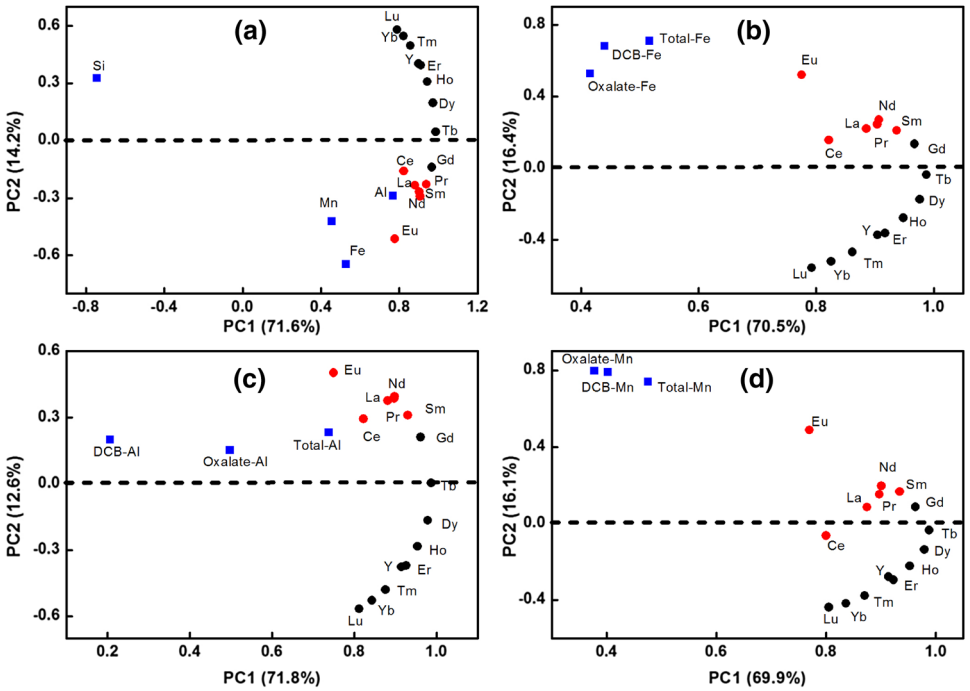

Fig. 4 A principal component analysis of REE contents with soil Fe, Al, Si, and Mn minerals. The oxalate- and DCB-extracted element contents were extracted with oxalic acid-ammonium oxalate (pH 3.2) and dithionite-citrate-bicarbonate (DCB) buffer solutions, respectively

and Si minerals, which suggests that the readily exchangeable REE pool was chiefly controlled by Fe minerals. LREE enrichment in soils resulted from their highly adsorptive affinity to mineral particles, whereas HREEs were preferentially retained in soil solutions (Compton et al. 2003; Yusoff et al. 2013).

4.2 Origin of Europium anomalies

All the studied soils from the PRD region exhibited a significant and negative Eu anomaly corresponding to the deep Eu "depression" of chondrite-normalized patterns (Fig. 2). The Eu/Eu* values of the total soil digestion, oxalate-, and DCB-extracts ranged 0.17–0.79 (mean of 0.55, n = 196), 0.15–1.62 (mean of 0.58), and 0.20–0.92 (mean of 0.60), respectively. Overall, the negative Eu anomalies were common characteristics of Eu distribution, and the Eu in the total digestion of soils was generally more pronounced than that of the partial extracts (Fig. 2).

The negative Eu anomaly in the soils generally resulted from the integrated factors of the sub-tropical climate and the soil secondary minerals. The formation of a Eu "depression" underwent three stages. First, the high temperature, rainy climate, and low soil pH in the PRD strengthened the mineral weathering and element leaching, which resulted in the formation of more active REEs. This stage was responsible for the foundation of REE fractionation (Huang et al. 2008). Then, in addition to the further weathering and leaching reactions, the mobile elements were intensively leached, during which the Fe-, Al-, and Mn-oxides accumulated and the according secondary minerals were generated continually. REEs, especially LREEs, therefore, were enriched in the secondary minerals of Fe-, Mn-, and Al-oxides (Tables S2, S3). Finally, Eu, as a valence-variable element, would have been easily reduced from Eu^{3+} to Eu^{2+} and leached in association with the further weathering processes of soil minerals (Liu et al. 2013; Condie et al. 1995). Fe- and Mn-oxides in the total soil digestion and partial extracts showed a significant positive correlation to the total Eu/Eu* ($p < 0.01$), and the Al oxides showed weaker or no correlation. This finding implies that the Eu^{3+} reduction was primarily dependent on Fe- and Mn-bearing minerals. The soil total Sr contents exhibited positive significant correlations to both total Eu contents and Eu/Eu* ($p < 0.01$) with correlation coefficients of 0.544 and 0.384, respectively. Eu^{2+} and Sr^{2+} have similar ionic radii (approximately 1.2 Å), and Sr^{2+} is easily leached into the soil solution (Lim et al. 2015). Eu would be easily leached together with Sr after being reduced from Eu^{3+} to Eu^{2+}, resulting in the co-leaching of Eu^{2+} and Sr (Fig. 5).

Total and partial soil extracts are highly negatively correlated with Eu anomalies, indicating that Eu was preferentially conveyed to the subsoil or another substance in the soil system. Comparing the Eu anomaly in the partial extracts with that in the corresponding total soil digestion can provide a valuable method for evaluating the relative mobility of Eu in the soils (Fig. 6). For example, if the total

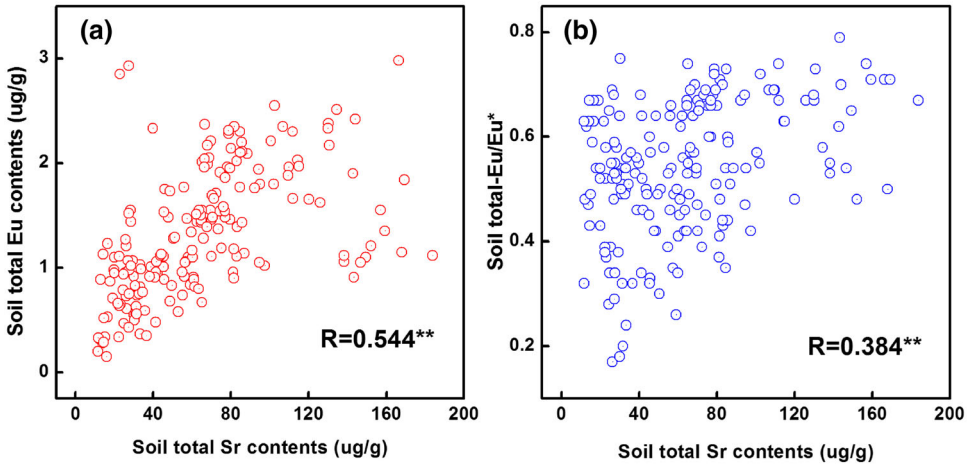

Fig. 5 Scatter plots of total soil strontium (Sr) versus europium (Eu) contents (**a**) and Eu/Eu* (**b**). The Pearson correlation coefficient and significance at the 0.01 level (2-tailed) are marked as "R" and "**" in each diagram

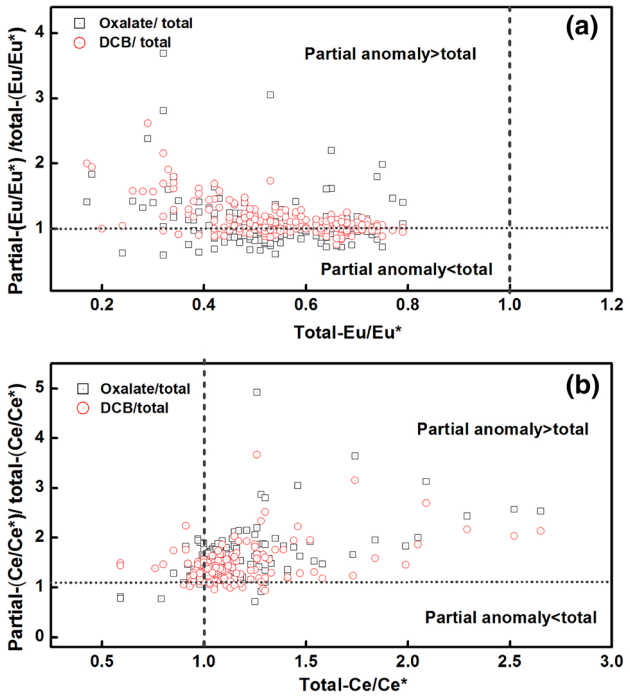

Fig. 6 Bivariate plots of Eu/Eu* (total digestion/partial extractions) versus Eu/Eu* in the total digestion (**a**) and Ce/Ce* (total digestion/partial extractions) versus Ce/Ce* in the total digestion (**b**). The oxalate- and DCB-extracted REE contents were extracted with oxalic acid-ammonium oxalate (pH 3.2) and citrate-bicarbonate-dithionite buffer solutions (DCB), respectively

digestion of the soils had a Eu/Eu* lower than 1 and the ratio of Eu anomaly in the partial extracts to Eu anomaly in the total digestion is higher than 1, the partial extract would have a less negative Eu anomaly than that in the total digestion (Fig. 6). Furthermore, Eu in most of the soils was more difficult to sequester into a more stable phase than Sm and Gd, which were preferentially extracted by the oxalate or DCB solutions. On the contrary, although the Eu anomaly ratio in the partial extracts to the total digests in some soils was <1, the Eu/Eu* in the total digestion was <1.

4.3 Origin of Cerium anomalies

The Ce in most of the soils exhibited a slightly positive anomaly, and also exhibited small Ce convex-up chondrite-normalized patterns (Fig. 3). The Ce/Ce* values of total soil digestion, oxalate-, and DCB-extracts ranged from 0.59 to 2.65 (mean δCe of 1.13, n = 196), 0.46 to 6.71 (mean Ce/Ce* of 1.87), and 0.85 to 5.66 (mean Ce/Ce* of 1.65), respectively, indicating that a positive Ce anomaly was a common characteristics in the PRD region. The partial analyses were generally more pronounced in the total extracts (Figs. 3l, 2).

In contrast to Eu, Ce^{3+} was readily oxidized into Ce^{4+} in the soil solution, which would be further co-precipitated with Fe/Mn (hydr)oxides and form CeO_2 or $Ce(OH)_4$ (Marker and De Oliveira 1990). These Ce species were insoluble and would be enriched in the soil secondary minerals, which consequently resulted in a positive Ce anomaly. Mn (hydr)oxides in the soil total digestion and partial extracts both showed significant negative correlations to the total Ce/Ce* ($p < 0.01$), and the Fe and Al (hydr)oxides showed no significant correlation to the total Ce/Ce*. These findings suggest that the oxidation of Ce^{3+} primarily resulted from reacting with soil Mn (hydr)oxides. In other words, the Mn minerals were primarily responsible for the Ce co-precipitation.

Comparing the Ce anomaly in the partial extracts with that in the corresponding total soil digestion shows the Ce in most soils was less mobile than Sm and Gd. The Ce/Ce* ratio in the partial extracts to the Ce/Ce* in the total digestion is higher than 1, indicating that the partial extract had a more positive Ce anomaly than that in the total digestion (Fig. 4) Moreover, the sample points in Fig. 4 from the first quadrant for axes X = 1 and Y = 1 (ratio of

partial -Ce/Ce* > 1 and total -Ce/Ce* > 1) indicate that Ce was less mobile than Sm and Gd and would be more easily sequestered into a different phase than Sm and Gd.

5 Conclusions

The chondrite-normalized REE patterns of the total values in the soils and partial extracts of the soils from the PRD region were similar, with a right-inclined pattern and LREE enrichment, a clear negative Eu anomaly, and a slightly positive Ce anomaly. Soil Fe and Mn minerals were found to be the primary minerals affecting REE distribution. Due to the higher adsorptive affinity of LREEs to soil mineral lattice than that of HREEs, fractionation between LREEs and HREEs occurred in different soils over the river delta region. In addition to soil minerals affecting REE fractionation, the active geochemical processes in soils in this region (e.g. soil redox-reaction processes) were probably responsible for the negative Eu anomaly and positive Ce anomaly, leading to the reduction of Eu^{3+} producing more leachable Eu^{2+} and oxidation of Ce^{3+} producing more readily precipitating Ce^{4+}.

Acknowledgments This work was funded by the National Natural Science Foundation of China (41420104007, 41330857, and 41673135), the Guangdong Natural Science Foundation of China (S2013050014266), and the One Hundred Talents Programme of The Chinese Academy of Sciences.

Compliance with ethical standards

Conflicts of interest The authors declare no conflicts of interest.

References

Babechuk MG, Widdowson M, Kamber BS (2014) Quantifying chemical weathering intensity and trace element release from two contrasting basalt profiles, Deccan Traps, India. Chem Geol 363:56–75

Banfield JF, Eggleton RA (1989) Apatite replacement and rare earth mobilization, fractionation, and fixation during weathering. Clays Clay Miner 37:113–127

Berger A, Janots E, Gnos E, Frei R, Bernier F (2014) Rare earth element mineralogy and geochemistry in a laterite profile from Madagascar. Appl Geochem 41:218–228

Boynton WV (1984) Cosmochemistry of the rare earth elements: meteorite studies. In: Henderson P (ed) Rare earth elements geochemistry. Elsevier, Amsterdam, pp 63–114

Braun J, Viers J, Dupré B, Polve M, Ndam J, Muller J (1998) Solid/liquid REE fractionation in the lateritic system of Goyoum, East Cameroon: the implication for the present dynamics of the soil covers of the humid tropical regions. Geochim Cosmochim Acta 62:273–299

Brioschi L, Steinmann M, Lucot E, Pierret MC, Stille P, Prunier J, Badot PM (2013) Transfer of rare earth elements (REE) from natural soil to plant systems: implications for the environmental availability of anthropogenic REE. Plant Soil 366:143–163

Caggianelli A, Fiore S, Mongelli G, Salvemini A (1992) REE distribution in the clay fraction of pelites from the southern Apennines, Italy. Chem Geol 99(4):253–263

Chen BH, Chen ZC, Liang QY, Fu QC, Yu SJ, Zhang LJ (1996) Compounding pattern of REE, clay and humic acid in the weathering crust of granites. J Rare Earth 14:47–53

Clark AM (1984) Mineralogy of the rare earth elements. In: Henderson P (ed) Rare earth elements geochemistry. Elsevier, Amsterdam, pp 33–61

Compton JS, White RA, Smith M (2003) Rare earth element behavior in soils and salt pan sediments of a semi-arid granitic terrain in the Western Cape, South Africa. Chem Geol 201:239–255

Condie KC, Dengate J, Cullers RL (1995) Behavior of rare earth elements in a paleoweathering profile on granodiorite in the Front Range, Colorado, USA. Geochim Cosmochim Acta 59:279–294

Cullers RL, Barrett T, Carlson R, Robinson B (1987) Rare-earth element and mineralogic changes in Holocene soil and stream sediment: a case study in the Wet Mountains, Colorado, USA. Chem Geol 63:275–297

Daux V, Crovisier JL, Hemond C, Petit JC (1994) Geochemical evolution of basaltic rocks subjected to weathering: fate of the major elements, rare earth elements, and thorium. Geochim Cosmochim Acta 58:4941–4954

Davranche M, Pourret O, Gruau G, Dia A (2004) Impact of humate complexation on the adsorption of REE onto Fe oxyhydroxide. J Colloid Interface Sci 277:271–279

Ettler V (2016) Soil contamination near no-ferrous metal surface: a review. Appl Geochem 64:56–74

Feng JL (2010) Behaviour of rare earth elements and yttrium in ferromanganese concretions, gibbsite spots, and the surrounding terra rossa over dolomite during chemical weathering. Chem Geol 271:112–132

Galán E, Fernández-Caliani JC, Miras A, Aparicio P, Márquez MG (2007) Residence and fractionation of rare earth elements during kaolinization of alkaline peraluminous granites in NW Spain. Clay Miner 42:341–352

Gruau G, Dia A, Olivié-Lauquet G, Davranche M, Pinay G (2004) Controls on the distribution of rare earth elements in shallow groundwaters. Water Res 38:3576–3586

Gurumurthy GP, Balakrishna K, Tripti M, Riotte J, Audry S, Bruan J, Shankar HNU (2015) Use of Sr isotopes as a tool to decipher the soil weathering processes in a tropical river catchment, south-western India. Appl Geochm 63:498–506

Hedrick JB (1995) The global rare-earth cycle. J Alloys Compd 225:609–618

Henderson P (1984) General geochemical properties and abundances of the rare earth elements. In: Henderson P (ed) Rare earth elements geochemistry. Elsevier, Amsterdam, pp 1–32

Holser WT (1997) Evaluation of the application of rare-earth elements to paleoceanography. Palaeogeogr Palaeoclimatol 132:309–323

Huang L, Hong J, Tan WF, Hu HQ, Liu F (2008) Characteristics of micromorphology and element distribution of iron–manganese cutans in typical soils of subtropical China. Geoderma 146:40–47

Kanazawa Y, Kamitani M (2006) Rare earth minerals and resources in the world. J Alloys Compd 408–412:1339–1343

Kissao G, Heinz JT (2003) Distribution patterns of rare-earth elements and uranium in tertiary sedimentary phosphorites of Hahotoé–Kpogamé, Togo. J Afr Earth Sci 37:1–10

Laveuf C, Cornu S (2009) A review on the potentiality of rare earth elements to trace pedogenetic processes. Geoderma 154:1–12

Lee S, Lee D, Kim Y, Chae B, Kim W, Woo N (2003) Rare earth elements as indicators of groundwater environment changes in a

fractured rock system: evidence from fracture-filling calcite. Appl Geochem 18:135–143
Leybourne MI (2001) Mineralogy and geochemistry of suspended sediments from groundwaters associated with undisturbed Zn-Pb massive sulfide sediments, Bathurst mining camp, New Brunswick, Canada. Can Miner 39:1597–1616
Leybourne MI, Johannesson KH (2008) Rare earth elements (REE) and yttrium in stream waters, stream sediments, and Fe–Mn oxyhydroxides: fractionation, speciation, and controls over REE + Y patterns in the surface environment. Geochim Cosmochim Acta 72:5962–5983
Li M, Xu RS, Ma YL, Zhu ZY, Wang J, Cai R, Chen Y (2008) Geochemistry and biogeochemistry of rare earth elements in a surface environment (soil and plant) in South China. Environ Geol 56:225–235
Lim D, Jung H, Xu Z, Jeong K, Li T (2015) Elemental and Sr–Nd isotopic compositional disparity of riverine sediments around the Yellow Sea: constraints from grain-size and chemical partitioning. Appl Geochem 63:272–281
Liu WJ, Liu CQ, Zhao ZQ, Xu ZF, Liang CS, Li LB, Feng JY (2013) Elemental and strontium isotopic geochemistry of the soil profiles developed on limestone and sandstone in karstic terrain on Yunnan-Guizhou Plateau, China: implications for chemical weathering and parent materials. J Asian Earth Sci 67–68:138–152
Liu F, Miao L, Cai G, Yan W (2015) The rare earth element geochemistry of surface sediments in four transects in the South China Sea and its geological significance. Environ Earth Sci 74:2511–2522
López JMG, Bauluz B, Fernández-Nieto C, Oliete AY (2005) Factors controlling the trace-element distribution in fine-grained rocks: the Albian kaolinite-rich deposits of the Oliete Basin (NE Spain). Chem Geol 214:1–19
Ma L, Jin LX, Brantley SL (2011) How mineralogy and slope aspect affect REE release and fractionation during shale weathering in the Susquehanna/Shale Hills critical zone observatory. Chem Geol 290:31–49
Marker A, De Oliveira JJ (1990) The formation of rare earth element scavenger minerals in weathering products derived from alkaline rocks of SE-Bahia, Brazil. Chem Geol 84:373–374
Marmolejo-Rodríguez AJ, Prego R, Meyer-Willerer A, Shumilin E, Sapozhnikov D (2007) Rare earth elements in iron oxyhydroxide rich sediments from the Marabasco River-Estuary system (pacific coast of Mexico). REE affinity with iron and aluminium. J Geochem Explor 94:43–51
Marsac R, Davranche M, Gruau G, Dia A, Pédrot M, Le Coz-Bouhnik M, Briant N (2013) Effects of Fe competition on REE binding to humic acid: origin of REE pattern variability in organic waters. Chem Geol 342:119–127
McLennan SM (1989) Rare earth elements in sedimentary rocks: influence of provenance and sedimentary processes. Rev Miner Geochem 21:169–200
Mehra OP, Jackson ML (1958) Iron oxide removal from soils and clays by a dithionite-citrate system buffered with sodium bicarbonate. Clays Clay Miner 7:317–327
Migaszewski Z, Galuszka A, Dolegowska S, Halas S, Krzciuk K, Gebus B (2015) Assessing the impact of Serwis mine tailings site on farmers' wells using element and isotope signatures (Holy Cross Mountains, South-Central Poland). Environ Earth Sci 74:629–647
Mongelli G, Cullers RL, Muelheisen S (1996) Geochemistry of late cretaceous - oligocenic shales from the varicolori formation, Southern Apennines, Italy: implications for mineralogical, grain-size control and provenance. Eur J Mineral 8(4):733–754
Ndjigui PD, Bilong P, Bitom D, Dia A (2008) Mobilization and redistribution of major and trace elements in two weathering profiles developed on serpentinites in the Lomié ultramafic complex, South-East Cameroon. J Afr Earth Sci 50:305–328
Nesbitt HW (1979) Mobility and fractionation of rare earth elements during weathering of a granodiorite. Nature 279:206–210
Öhlander B, Land M, Ingri J, Widerlun A (1996) Mobility of rare earth elements during weathering of till in northern Sweden. Appl Geochem 11:93–99
Ohta A, Kawabe I (2001) REE(III) adsorption onto Mn dioxide (δ-MnO_2) and Fe oxyhydroxide: ce(III) oxidation by δ-MnO_2. Geochim Cosmochim Acta 65:695–703
Pansu M, Gautheyrou J (2006) Handbook of soil analysis: mineralogical, organic and inorganic methods. Springer, Dordrecht
Peretyazhko T, Sposito G (2005) Iron(III) reduction and phosphorous solubilization in humid tropical forest soils. Geochim Cosmochim Acta 69:3643–3652
Pourret O, Davranche M, Dia Gruau GA (2007) Rare earth elements complexation with humic acid. Chem Geol 243:128–141
Ren L, Cohen DR, Rutherford NF, Zissimos AM, Morisseau EG (2015) Reflections of the geological characteristics of Cyprus in soil rare earth element patterns. Appl Geochem 56:80–93
Sanematsu K, Kon Y, Imai A, Watanabe K, Watanabe Y (2013) Geochemical and mineralogical characteristics of ion-adsorption type REE mineralization in Phuket, Thailand. Miner Depos 48:437–451
Schwertmann U (1964) Differenzierung der Eisenoxide des Bodens durch Extraktion mit Ammoniumoxalat-Lösung. J Plant Nutr Soil Sci 105:194–202
Singh P, Rajamani V (2001) REE geochemistry of recent clastic sediments from the Kaveri floodplains, southern India: implication to source area weathering and sedimentary processes. Geochim Cosmochim Acta 65(18):3093–3108
Šmuc NR, Dolenec T, Serafimovski T, Dolenec M, Vrhovnik P (2012) Geochemical characteristics of rare earth elements (REEs) in the paddy soil and rice (*Oryza sativa* L.) system of Kočani Field Republic of Macedonia. Geoderma 183–184:1–11
Soil Survey Staff (2004) Soil Survey Laboratory Methods Manual. Soil Survey Investigation Report No. 42. Version 4.0. US Govt. Print. Off, Washington, DC
Sonke JE (2006) Lanthanide—humic substances complexation. II. Calibration of humic ion-binding model V. Environ Sci Technol 40:7481–7487
Takahashi Y, Yoshida H, Sato N, Hama K, Yusa Y, Shimizu H (2002) W- and M-type tetrad effects in REE patterns for water–rock systems in the Tono uranium deposit, central Japan. Chem Geol 184:311–335
Tani Y, Miyata N, Iwahori K, Soma M, Tokuda S, Seyama H, Theng BKG (2003) Biogeochemistry of manganese oxide coatings on pebble surfaces in the Kikukawa River System, Shizuoka, Japan. Appl Geochem 18:1541–1554
Taunton AE, Welch SA, Banfield JF (2000) Microbial controls on phosphate and lanthanide distributions during granite weathering and soil formation. Chem Geol 169:371–382
Wayne NH, Markovics G (1997) Weathering of granodioritic crust, long-term storage of elements in weathering profiles, and petrogenesis of siliciclastic sediments. Geochim Cosmochim Acta 61:1653–1670
Wei ZG, Yin M, Zhang X, Hong FS, Li B, Tao Y, Zhao GW, Yan CH (2001) Rare earth elements in naturally grown fern Dicranopteris linearis in relation to their variation in soils in South-Jiangxi region (Southern China). Environ Pollut 114:345–355
Xing XW, Ye JF, Ou WD, Peng QP, Zhu SW, Liu ZH, Gao JS (2012) Guangdong statistical yearbook—2012. China Statistical Press, Statistics Bureau Of Guangdong Province, Guangzhou, pp 111–222
Yan B, Yan W, Miao L, Huang W, Chen Z (2012) Geochemical characteristics and provenance implication of rare earth elements

in surface sediments from bays along Guangdong Coast, Southeast China. Environ Earth Sci 65:2195–2205

Yang YG, Liu CQ, He ZL, Yuan KN (2004) Rare earth element (REE) geochemistry during red soil formation in Southern China. In: Wilson MJ, He ZL, Yang XE (eds) The red soils of China. Springer, New York, pp 89–100

Yusoff ZM, Ngwenya BT, Parsons I (2013) Mobility and fractionation of REEs during deep weathering of geochemically contrasting granites in a tropical setting, Malaysia. Chem Geol 349–350:71–86

Zhu JG, Xing GX (1992) Forms of Rare Earth Elements in Soils: Differentiation of Rare Earth Elements. Pedosphere 2:193–200